Substrate Integrated Waveguide Leaky-Wave Antenna With H-Shaped Slots

Juhua Liu, Xihui Tang, Yuanxin Li, and Yunliang Long

***Abstract*—A new leaky-wave antenna based on substrate integrated waveguide (SIW) with H-shaped slots is proposed and investigated. The SIW with H-shaped slots is analyzed as a rectangular waveguide with H-shaped slots. Using an aperture magnetic field integral equation (MFIE), it is found that the SIW with H-shaped slots supports a leaky waveguide mode, a surface-wave mode and a proper waveguide mode depending on frequency. The radiation property is also evaluated using the MFIE. The leaky-wave antenna based on the SIW with H-shaped slots has a narrow beam that scans from broadside to endfire with frequency. The antenna produces an elliptical polarization, including circular polarization. Measured results are consistent with the simulation from HFSS and the theoretical analysis from the MFIE.**

***Index Terms*—Elliptical polarization, leaky-wave antenna, magnetic field integral equation, substrate integrated waveguide (SIW).**

I. Introduction

Substrate integrated waveguide (SIW) has attracted extensive attention in recent years [1], [2] for its significant advantages of low profile, low cost, and easy integration with microstrip or coplanar circuit. The SIW has been used to design leaky-wave antennas [3]–[10]. The SIW leaky-wave antennas have a simple structure and produce a narrow beam that scans with frequency. Leaky-wave antennas mostly produce a linear polarization.

Two leaky-wave antennas that could provide a circular polarization were published previously [11], [12]. But these circularly polarized antennas need a feeding network with a phase difference of 90° to support the radiation elements.

In the last century, W. J. Getsinger proposed an elliptically polarized leaky-wave antenna based on a rectangular waveguide with cross slots [13]. This type of leaky-wave antenna has a simple structure and is easy to feed. It produces a beam that has an elliptical polarization, including circular polarization [13]. However, the cross-slotted rectangular waveguide with air-filling can not scan to endfire, because the phase constant of the guided wave can not reach or exceed the wavenumber in free space.

In this communication, we propose a new elliptically polarized leaky-wave antenna based on an SIW with H-shaped slots (Fig. 1). The antenna can scan well from broadside to endfire, as opposed to the SIW leaky-wave antenna with transverse slots that can not radiate well near broadside [10], [14], [15] and the SIW leaky-wave antenna with longitudinal slots that can not scan to endfire due to the polarization of the radiating equivalent magnetic currents. The proposed antenna has a similar property of the elliptically polarized leaky-wave antenna based on the air-filled rectangular waveguide with cross slots [13]. However, compared to the air-filled rectangular waveguide with cross slots [13], the dielectric filling (substrate) in the SIW makes an important difference since it allows for the beam to scan to endfire, and the SIW is easier to fabricate than the rectangular waveguide. Moreover, it is much easier to obtain a high leakage using H-shaped slots than using cross slots.

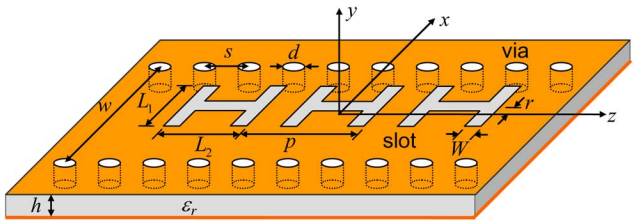

Fig. 1. The geometry of the SIW with H-shaped slots. The SIW has $w = 10.5$ mm, $\varepsilon_r = 2.25$, $h = 1$ mm, $d = 0.8$ mm, and $s = 1.6$ mm. The slots have $L_1 = 4.6$ mm, $L_2 = 4.1$ mm, $W = 0.45$ mm, and $p = 6$ mm, $r = 0.45$ mm.

Since an SIW can be considered as a rectangular waveguide [1], [2], the SIW with H-shaped slots can be analyzed as a dielectric-filled rectangular waveguide with H-shaped slots. In this communication, we use a magnetic field integral equation (MFIE) [16] to investigate the modes propagating in the rectangular waveguide with H-shaped slots. The dielectric-filled rectangular waveguide with H-shaped slots supports a leaky waveguide mode, a surface-wave mode and a proper waveguide mode. The wavenumber of the SIW with H-shaped slots is also evaluated by HFSS and compared with the results from the MFIE. An excellent agreement is obtained between the results from HFSS and those from the MFIE. Besides, the polarization of the SIW with H-shaped slots is also analyzed with the MFIE and validated with the simulation by HFSS. The polarization depends on the shape and position of the H-shaped slots and changes with frequency.

A leaky-wave antenna based on SIW with H-shaped slots is designed that has a simple structure and is fed with a microstrip line. A prototype is fabricated, and measured results are consistent with the simulation and the theoretical analysis. This antenna has a wide impedance bandwidth and a narrow beam that scans from broadside to endfire with frequency. An elliptical polarization is produced and a circular polarization can even be achieved. This type of leaky-wave antenna can be potentially used to microwave and millimeter-wave systems that need an antenna with beam-scanning ability [17] or with a narrow beam with circular polarization [13].

II. Theory

A. MFIE

The geometry of the SIW with H-shaped slots is shown in Fig. 1. The SIW is constructed on a wide microstrip line that is shorted at the edges with conductive vias, acting as a rectangular waveguide. The width and height of the SIW are w and h respectively. The substrate has a dielectric constant ε_r. The diameter of the via and the distance between two vias are d and s, respectively. Leakage is obtained by introducing a periodic set of H-shaped slots on the top of the SIW. The transverse and longitudinal slots of the H-shaped slot have lengths L_1 and L_2, and an identical width W, as shown in Fig. 1. Note that the center of the H-shaped slot is at a distance of r from the z axis. The period of the H-shaped slots is p.

The SIW with H-shaped slots is analyzed as an equivalent dielectric-filled rectangular waveguide with H-shaped slots. Suppose the rectangular waveguide has a width of a and a height of b. The width a of the rectangular waveguide is the equivalent width of the SIW [2]. For

Manuscript received May 16, 2011; revised February 02, 2012; accepted March 03, 2012. Date of publication May 23, 2012; date of current version July 31, 2012. This work was supported in part by the Natural Science Foundation of China under Grants 60901028 and 61172026, the Fundamental Research Funds for the Central Universities, and in part by NSFC-Guangdong under Grant U0935002.

The authors are with the Department of Electronics & Communication Engineering, Sun Yat-sen University, Guangzhou, China (e-mail: liujuhua_2000@hotmail.com; isslyl@mail.sysu.edu.cn).

Color versions of one or more of the figures in this communication are available online at http://ieeexplore.ieee.org.

Digital Object Identifier 10.1109/TAP.2012.2201085

the SIW with the parameters given in Fig. 1, the equivalent width of the SIW is $w_{eff} = 9.9842$ mm [2]. The height b of the waveguide is exactly the height h of the SIW. To simplify the analysis, it is assumed that the waveguide is infinitely long and the top wall is extended into an infinite ground plane, as assumed in [16]. The metal is assumed lossless in this investigation, and the thickness of the waveguide wall is assumed infinitesimal.

The dielectric-filled rectangular waveguide with H-shaped slots is analyzed using the MFIE described in [16]. Owing to the periodicity of the structure, the analysis is restricted to only one spatial period (unit cell). The tangential electric field on the aperture is equated to an equivalent magnetic current $\mathbf{M}$. Enforcing continuity for the tangential magnetic fields across the slot boundary yields an integral equation. The integral equation is solved by a method of moments, in which a rectangular mesh is adopted and the equivalent magnetic current density on the zeroth slot is expanded on a set of rooftop basis functions

$$\mathbf{M}(x,z) = \hat{x}\sum_{v=1}^{V_x} c_v \Lambda_{xv}(x) + \hat{z}\sum_{v=1}^{V_z} d_v \Lambda_{zv}(z) \tag{1}$$

where the definitions of the rooftop functions Λ_{xv} and Λ_{zv} are given in [16]. More complete description of the method is found in [16].

B. Far Field

When the magnetic current distribution on the aperture is solved with the MoM, the far field can be calculated. The calculation of radiation patterns was not discussed in [16]. In this subsection equations for calculating the far fields will be given.

In our calculation, only the magnetic fields M_x and M_z need to be considered. According to [18], the far fields can be calculated by

$$\begin{cases} E_\theta = -jk_0 \frac{1}{4\pi r} e^{-jk_0 r} L_\phi \\ E_\phi = jk_0 \frac{1}{4\pi r} e^{-jk_0 r} L_\theta \end{cases} \tag{2}$$

where

$$\begin{cases} L_\phi = -L_x \sin\phi \\ L_\theta = L_x \cos\theta\cos\phi - L_z \sin\theta \end{cases}. \tag{3}$$

If a leaky-wave antenna has a series of N identical H-shaped slots on the top wall of the rectangular waveguide and the antenna is assumed to have only a forward traveling wave with a wavenumber $k_z = \beta - j\alpha$, the functions L_x and L_z in (3) can be calculated by

$$\begin{cases} L_x = \sum_{n=1}^{N}\sum_{v=1}^{V_x} c_v L_x^{(v,n)} \\ L_z = \sum_{n=1}^{N}\sum_{v=1}^{V_z} d_v L_z^{(v,n)} \end{cases} \tag{4}$$

where, see (5), shown at the bottom of page, and

$$\begin{aligned} L_z^{(v,n)} &= 2\Delta x_u \operatorname{sinc}\left(\frac{\Delta x_u k_0 \sin\theta\cos\phi}{2}\right) \\ &\cdot \frac{\left(\Delta z_v^+ + \Delta z_v^- - \Delta z_v^+ e^{jk_0\cos\theta\cdot\Delta z_u^-} - \Delta z_v^- e^{-jk_0\cos\theta\cdot\Delta z_v^+}\right)}{(k_0\cdot\cos\theta)^2 \Delta z_v^+ \Delta z_v^-} \\ &\cdot e^{jnp(k_0\cos\theta - k_z) + jx_u k_0 \sin\theta\cos\phi + jk_0 z_u\cos\theta}. \end{aligned} \tag{6}$$

C. Polarization Ratio

If the attenuation constant α is very small compared to the phase constant β, or $k_z \approx \beta$, the main beam radiation angle θ_0 can be calculated by $\cos\theta_0 \approx \beta/k_0$ [19]. The polarization ratio at the radiation angle ($\phi = 90^\circ$, $\theta = \theta_0$) can then be calculated by

$$\begin{aligned} \frac{E_\phi}{E_\theta} &= -\frac{\sqrt{k_0^2 - \beta^2}}{k_0} \\ &\cdot \frac{\sum_{v=1}^{V_z} d_v \Delta x_v \frac{\Delta z_v^+ + \Delta z_v^- - \Delta z_v^+ e^{j\beta\Delta z_u^-} - \Delta z_v^- e^{-j\beta\Delta z_v^+}}{\beta^2 \Delta z_v^+ \Delta z_v^-} \cdot e^{j\beta z_u}}{\sum_{v=1}^{V_x} c_v \Delta z_v \operatorname{sinc}\left(\frac{\beta\Delta z_v}{2}\right) \cdot \frac{\Delta x_v^- + \Delta x_v^+}{2} \cdot e^{j\beta z_v}}. \end{aligned} \tag{7}$$

III. Numerical Results

A. Propagation Characteristics

Using the MFIE described in [16], the normalized phase and leakage (attenuation) constants for the equivalent rectangular waveguide with H-shaped slots are calculated and shown in Fig. 2 and Fig. 3. Results for the corresponding closed rectangular waveguide are also shown for comparison. Very similar to the modes in a dielectric-filled rectangular waveguide with transverse slots [10], three modes are found in the dielectric-filled rectangular waveguide with H-shaped slots. In Fig. 2, solution (a) is a leaky waveguide mode that is an attenuated and improper mode, solution (b) is a surface-wave mode that is a bound and proper mode, and solution (c) is a proper waveguide mode. More complete descriptions of these modes can be found in [10].

The wavenumber for the SIW with H-shaped slots can be extracted from HFSS [10]. Fig. 2 and Fig. 3 show that the results from HFSS for the SIW with H-shaped slots agree very well with the wavenumbers calculated from the MFIE for the equivalent rectangular waveguide with H-shaped slots. Therefore, the SIW with H-shaped slots can be well considered as a rectangular waveguide with H-shaped slots.

The SIW with transverse slots [10] that only cut the longitudinal current J_z has a leakage constant that increases as frequency increases in the leaky region, and its leakage constant is almost zero at the cutoff frequency where it radiates at broadside. Thus the SIW leaky-wave antenna with transverse slots can not radiate well at broadside and near broadside [10]. On the other side, the SIW with longitudinal slots that only cut the transverse current J_x has a leakage constant that decreases

$$\begin{aligned} L_x^{(v,n)} &= 2\Delta z_u \operatorname{sinc}\left(\frac{k_0\cos\theta\cdot\Delta z_u}{2}\right) \\ &\cdot \frac{\Delta x_u^+ + \Delta x_u^- - \Delta x_u^+ e^{jk_0\Delta x_u^-\sin\theta\cos\phi} - \Delta x_u^- e^{-jk_0\Delta x_u^+\sin\theta\cos\phi}}{(k_0\sin\theta\cos\phi)^2 \Delta x_u^+ \Delta x_u^-} \\ &\cdot e^{jnp(k_0\cos\theta - k_z) + jk_0 x_u\sin\theta\cos\phi + jk_0 z_u\cos\theta} \end{aligned} \tag{5}$$

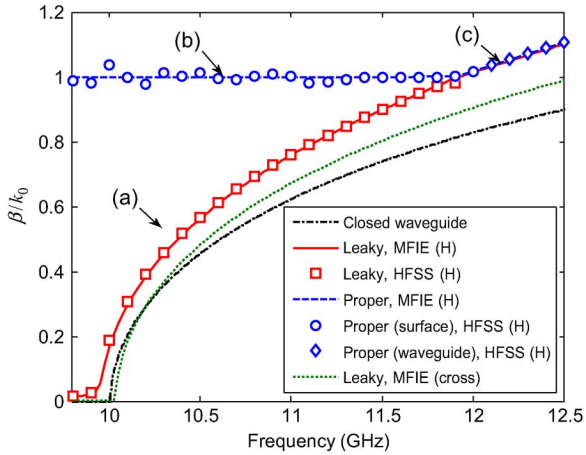

Fig. 2. Normalized phase constant for the SIW with H-shaped slots vs. frequency. The SIW with H-shaped slots has the dimensions given in Fig. 1. Normalized phase constant for the dielectric-filled rectangular waveguide with cross slots is also shown for comparison.

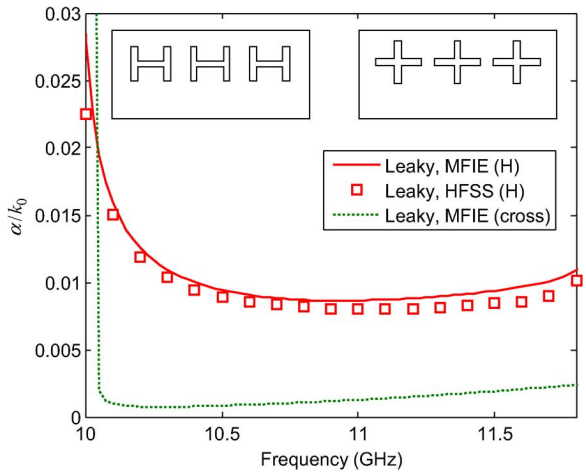

Fig. 3. Normalized leakage constant for the SIW with H-shaped slots vs. frequency. The SIW with H-shaped slots has the dimensions given in Fig. 1. Normalized leakage constant for the dielectric-filled rectangular waveguide with cross slots is also shown for comparison.

as frequency decreases, and it has a zero leakage constant when it radiates at endfire. Therefore the SIW leaky-wave antenna with longitudinal slots can not radiate well at endfire.

Since an H-shaped slot includes both transverse slots and longitudinal slot, the H-shaped slot cuts both the longitudinal current J_z and transverse current J_x on the rectangular waveguide. Therefore, the leakage constant of the SIW with H-shaped slots is relatively flat, and it is not zero when the antenna radiates at broadside ($\beta = \alpha$) or at endfire ($\beta = k_0$), so the SIW leaky-wave antenna can scan well from broadside to endfire.

Fig. 2 and Fig. 3 also show the normalized phase and leakage constants for a dielectric-filled rectangular waveguide with cross slots. The dielectric-filled rectangular waveguide with cross slots has the same dimensions of the dielectric-filled rectangular waveguide with H-shaped slots (the equivalent waveguide of the SIW with H-shaped slots). The transverse slot and longitudinal slot of the cross slot have an identical length $L = 4.6$ mm and an identical width $W = 0.45$ mm. The period and the center position of the cross slots are the same as those of the H-shaped slots. Here, only the leaky mode of the dielectric-filled

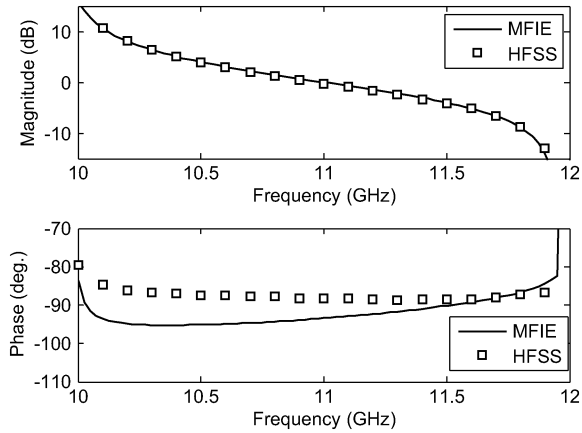

Fig. 4. Magnitude and phase of the ratio E_ϕ/E_θ at the radiation angle (the main beam of the total field) for an SIW leaky-wave antenna that has 42 identical H-shaped slots. The SIW with H-shaped slots has the dimensions given in Fig. 1.

rectangular waveguide with cross slots is shown for simplicity. Note that the dielectric-filled rectangular waveguide with cross slots also supports proper modes (including a surface-wave mode and a proper waveguide mode) that are similar to those in the dielectric-filled rectangular waveguide with H-shaped slots. Fig. 3 shows that the leakage constant of the dielectric-filled rectangular waveguide with cross slots is much smaller than that of the dielectric-filled rectangular waveguide with H-shaped slots, probably due to that the H-shaped slots cut the electric current more efficiently than do the cross slots.

B. Radiation Characteristics

Fig. 4 shows the polarization radio E_ϕ/E_θ at the radiation angle ($\phi = 90°$, $\theta = \theta_0$). The MFIE for calculating the ratio is discussed in Section II-C. Fig. 4 shows that the ratio simulated from HFSS for the SIW with H-shaped slots agrees very well with the one calculated from the MFIE for the equivalent slotted rectangular waveguide.

Fig. 4 shows that the magnitude of the radio E_ϕ/E_θ decreases with the increase of frequency. The magnitude of the radio E_ϕ/E_θ is between -6 dB and 6 dB in the band from 10.3 GHz to 11.6 GHz, and the phase of the radio E_ϕ/E_θ is close to $-90°$ in the band. The phase difference of the field components E_ϕ and E_θ should probably be due to that the transverse and longitudinal currents on the waveguide have a $90°$ phase difference. The antenna thus produces a right-hand circular polarization (RHCP) for the main beam. Fig. 4 shows that the antenna achieves a circular polarization at 10.9 GHz.

The ratio E_ϕ/E_θ can be changed by selection of the shape and position of the H-shaped slots. An increase of the transverse slot length L_1 has more current J_z cut, and the far field E_θ will increase and the ratio E_ϕ/E_θ will decrease accordingly. On the other hand, an increase of the longitudinal slot length L_2 or an increase of the distance r results in more current J_x being cut, and the far field E_ϕ will then increase and the ratio E_ϕ/E_θ will increase. When the H-shaped slots are placed at the center of the broad wall of the SIW ($r = 0$), the antenna will have the same radiation property of the SIW with transverse slots that only produces a linear far field E_θ.

The antenna investigated here is fed at the left port and the distance r is positive. Analysis shows that such antenna produces an RHCP. However, if r is negative and the antenna is fed at the left port, the antenna will produce a left-hand circular polarization (LHCP). If the antenna is fed at the right port, the antenna will radiate at backward quadrant, and will produce an LHCP for a positive value of r or an RHCP for a negative value of r. Therefore, this antenna can be designed to have an LHCP or an RHCP conveniently.

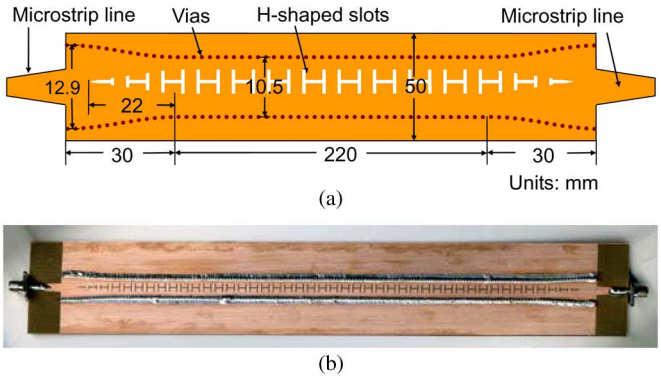

Fig. 5. The leaky-wave antenna based on SIW with H-shaped slots. The uniform portion of the slotted SIW has the same dimensions as in Fig. 1. The dielectric has a tangent loss of $\tan\delta = 0.001$ and the conductor has a conductivity of $\sigma = 5.8 \times 10^7$ S/m. The antenna is fed with a tapered microstrip line with a length of 15 mm and a width being linearly tapered from 4.7 mm to 3.1 mm. The length and width of the ground plane are 310.2 mm and 50 mm. (a) The geometry (not to scale). (b) The fabricated antenna.

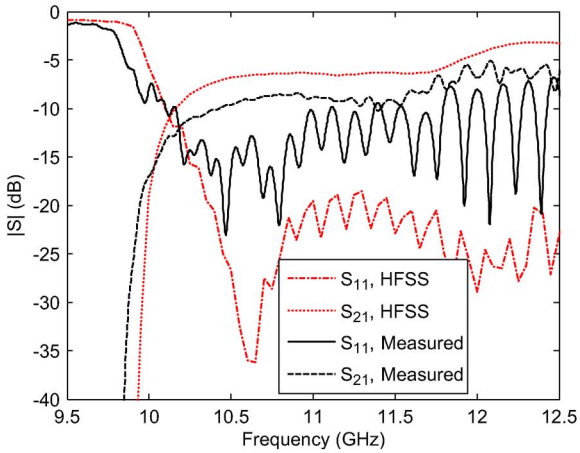

Fig. 6. S parameters for the SIW leaky-wave antenna shown in Fig. 5.

IV. Measurements

A. Geometry

Here, an SIW leaky-wave antenna is designed. The geometry of the antenna is shown in Fig. 5. The slotted SIW antenna is fed with a microstrip line. To enhance the impedance bandwidth, the SIW is tapered as a cosine function at both ends. In order to have a better match between the slotted SIW and the microstrip line, the H-shaped slots are tapered linearly at both ends, and the microstrip line are tapered linearly, as shown in Fig. 5. The dominant part of the antenna is an SIW with 220 mm that is etched with identical H-shaped slots.

B. S Parameters

The results for S_{11} and S_{21} are shown in Fig. 6. The simulated results from HFSS are very close to the measured ones. Measured results show that S_{11} is mostly less than -10 dB in the band from 9.9 GHz to 11.7 GHz. The measured result for S_{11} is a litter larger than the simulated one because the fabrication is not accurate enough and the loss from the SMA connectors is not included in the simulation. Measured results show that S_{21} is less than -8.4 dB in the band from 9.9 GHz to 11.5 GHz, meaning good load efficiency. Beyond 11.5 GHz, the antenna scans very close to endfire, and more and more power is transmitted into the terminated end but not radiated into space, so the S_{21} increases beyond 11.5 GHz. The measured S_{21} stops increasing when the frequency goes to about 11.8 GHz, meaning that very small power

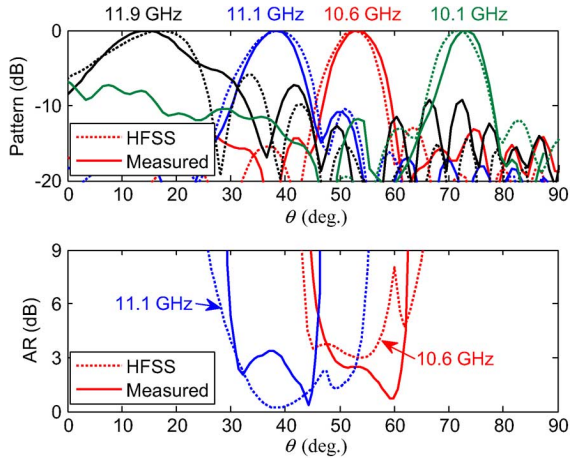

Fig. 7. Radiation patterns (RHCP) and axial ratios (AR) for the SIW leaky-wave antenna shown in Fig. 5. The frequencies given here are simulated ones. The measured frequencies are 0.2 GHz less than the corresponding simulated frequencies. The solid lines denote measured results while the dotted lines denote simulated results. Results for AR are only shown for the frequencies at 10.6 GHz and 11.1 GHz and for the angles nearby the main lobe.

is leaked into space. The simulated result for S_{21} is a little larger than the measured one, probably due to increased conductor and dielectric losses in the fabricated antenna. A frequency shift of about 0.2 GHz is observed between the simulated and the measured results, probably due to small errors in fabrication and an increased dielectric constant used in the experiment.

C. Radiations

The simulated and measured results for RHCP at simulated frequencies 10.1 GHz, 10.6 GHz, 11.1 GHz and 11.9 GHz are shown in Fig. 7. (Since the antenna produces a mainly RHCP, only the patterns for RHCP are shown here for simplicity.) Since a frequency shift of about 0.2 GHz occurs between the simulated and measured results, in order to have a better comparison, the simulated radiation patterns are compared with the measured ones that have a 0.2 GHz frequency shift. A very good agreement is observed between the simulated and measured results. It shows that the antenna scans from near broadside to near endfire with frequency.

The results for axial ratio (AR) at simulated frequencies 10.6 GHz and 11.1 GHz (corresponding to measured frequencies 10.4 GHz and 10.9 GHz) are shown. The measured AR has a small difference compared with the simulated one probably due to the errors in the fabrication and measurement. Measured results show that the antenna produces a circular polarization at 10.4 GHz and a near circular polarization at 10.9 GHz. It is seen that the best axial ratio may not coincidently appear at the direction of the main lobe, but at a direction with a little shift from the main lobe. This is probably due to that the E_ϕ has another factor "$\sin\theta$" compared with the E_θ in the main radiation plane ($\phi = 90^\circ$), with respect to (2) and (3). Error in the measurement may also have an effect on the non-coincidence. (At 10.1 GHz and 11.9 GHz where the antenna radiates at near broadside and near endfire, the AR is so high that the results are not shown for these frequencies.)

The radiation angle and AR for the main lobe are shown in Fig. 8 vs. frequency. The main beam scans from near broadside to near endfire as frequency increases. A frequency shift of about 0.2 GHz is observed between the simulated results and the measured ones. The simulated AR has the lowest level at 11.1 GHz, and a value less than 3 dB in the band from 10.7 GHz to 11.3 GHz and a value less than 6 dB in the band from 10.3 to 11.6 GHz. The measured AR is a little higher than the simulated one, and a shift of frequency is observed, probably due

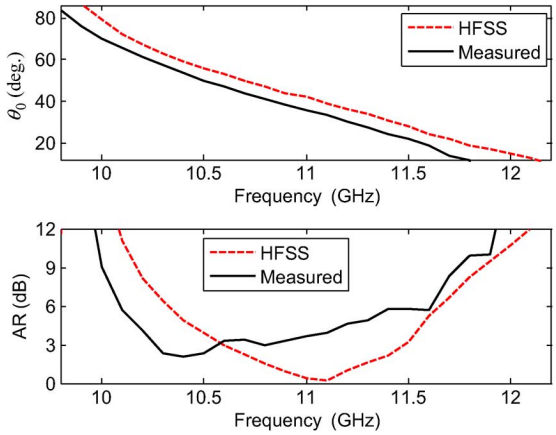

Fig. 8. Radiation angle θ_0 and axis ratio for the RHCP of the SIW leaky-wave antenna shown in Fig. 5.

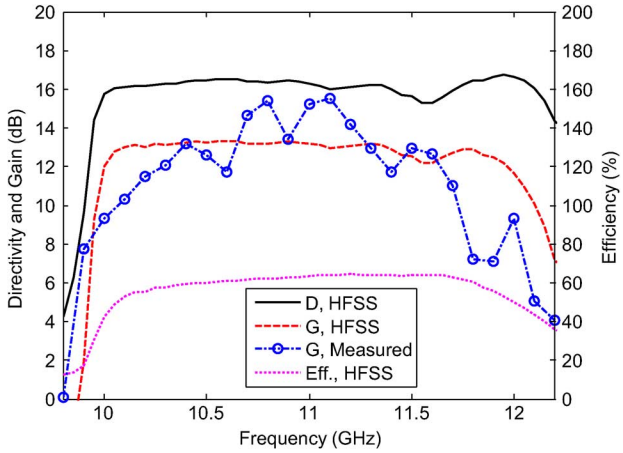

Fig. 9. Radiation efficiency, and directivity and gain for the RHCP of the SIW leaky-wave antenna shown in Fig. 5.

to the errors in the fabrication and measurement. The measured AR is less than 3 dB in the band from 10.3 GHz to 10.5 GHz, and is less than 6 dB in the band from 10.1 GHz to 11.3 GHz. The measured and simulated bands for $\mathrm{AR} \leq 6$ dB are close to the band from 10.3 GHz to 11.6 GHz in which the theoretical results in Section III-B show that the ratio E_ϕ / E_θ is between -6 dB and 6 dB. The level of 6 dB for the ratio $|E_\phi / E_\theta|$ was used previously in the research for the circular polarization property of the rectangular waveguide with cross-slots [13]. When the antenna radiates near broadside or near endfire, the radiation has a linear polarization, which is consistent with the numerical results in Section III-B.

D. Gain

Fig. 9 shows the directivity and gain for RHCP and the radiation efficiency. Measured results show that the antenna has a high gain in the band from 9.9 GHz to 11.7 GHz. It is observed that the measured gain is close to the simulated result. The measured gain drops at 11.8 GHz, where the antenna has passed the endfire radiation. The measured gain drops at a lower frequency than the simulated gain, probably due to a frequency shift and that the measured antenna suffers more from the finite ground diffraction effects [10]. Simulated results show that the gain is about 3 dB lower than the directivity, due to a radiation efficiency of about 0.6.

V. Conclusion

A novel leaky-wave antenna based on SIW with H-shaped slots is proposed. The SIW leaky-wave antenna has a narrow elliptically polarized beam that scans from broadside to endfire with frequency. Compared with cross slots, it is much easier to obtain a high leakage using the H-shaped slots.

The propagation characteristics and radiation properties are analyzed with an MFIE solved by an MoM. Theoretical analysis finds that the SIW with H-shaped slots supports a leaky waveguide mode, a surface-wave mode and a proper waveguide mode. The complex propagation wavenumber is calculated with the MFIE and validated with the simulation by HFSS. The radiation properties of the SIW with H-shaped slots are also analyzed with MFIE and validated with the simulation by HFSS. A uniform slotted leaky-wave antenna based on SIW with H-shaped slots is designed, and the measured results are consistent with the simulated results.

Acknowledgment

The authors wish to acknowledge Prof. D. R. Jackson, University of Houston, Houston, TX, and Prof. T. S. Bird, CSIRO ICT Centre, Australia, and the reviewers for their advice.

References

[1] F. Xu and K. Wu, "Guided-wave and leakage characteristics of substrate integrated waveguide," *IEEE Trans. Microwave Theory Tech.*, vol. 53, no. 1, pp. 66–73, Jan. 2005.

[2] L. Yan, W. Hong, K. Wu, and T. J. Cui, "Investigations on the propagation characteristics of the substrate integrated waveguide based on the method of lines," *Proc. Inst. Elect. Eng.—Microw. Antennas Propag.*, vol. 152, pp. 35–42, Feb. 2005.

[3] D. Deslandes and K. Wu, "Substrate integrated waveguide leaky-wave antenna: Concept and design considerations," presented at the Asia-Pacific Microwave Conf., Dec. 2005.

[4] F. Xu, K. Wu, and X. Zhang, "Periodic leaky-wave antenna for millimeter wave applications based on substrate integrated waveguide," *IEEE Trans. Antennas Propag.*, vol. 58, no. 2, pp. 340–347, Feb. 2010.

[5] J. Xu, W. Hong, H. Tang, Z. Kuai, and K. Wu, "Half-mode substrate integrated waveguide (HMSIW) leaky-wave antenna for millimeter-wave applications," *IEEE Antenna Wireless Propag. Lett.*, vol. 7, pp. 85–88, 2008.

[6] Q. Lai, C. Fumeaux, W. Hong, and R. Vahldieck, "Characterization of the propagation properties of the half-mode substrate integrated waveguide," *IEEE Trans. Microwave Theory Tech.*, vol. 57, no. 8, pp. 1996–2004, Aug. 2009.

[7] J. Machác, P. Lorenz, M. Sağlam, C. Bui, and W. Kraemer, "A substrate integrated waveguide leaky wave antenna radiating from a slot in the broad wall," in *Proc. IEEE Microwave Symp. Digest (MTT)*, 2010, pp. 5–8.

[8] Y. J. Cheng, W. Hong, K. Wu, and Y. Fan, "Millimeter-wave substrate integrated waveguide long slot leaky-wave antennas and two-dimensional multibeam applications," *IEEE Trans. Antennas Propag.*, vol. 59, no. 1, pp. 40–47, Jan. 2011.

[9] Y. Dong and T. Itoh, "Composite right/left-handed substrate integrated waveguide and half mode substrate integrated waveguide leaky-wave structures," *IEEE Trans. Antennas Propag.*, vol. 59, no. 3, pp. 767–775, Mar. 2011.

[10] J. Liu, D. R. Jackson, and Y. Long, "Substrate integrated waveguide (SIW) leaky-wave antenna with transverse slots," *IEEE Trans. Antennas Propag.*, vol. 60, no. 1, pp. 20–29, Mar. 2012.

[11] Y. Cheng, W. Hong, and K. Wu, "Millimeter-wave half mode substrate integrated waveguide frequency scanning antenna with quadri-polarization," *IEEE Trans. Antennas Propag.*, vol. 58, no. 6, pp. 1848–1855, Jun. 2010.

[12] Y. Li, Q. Xue, E. K. N. Yung, and Y. Long, "Circularly-polarized microstrip leaky-wave antenna," *Electron. Lett.*, vol. 43, no. 14, Jul. 2007.

[13] W. J. Getsinger, "Elliptically polarized leaky-wave array," *IRE Trans. Antennas Propag.*, vol. 165–171, Mar. 1962.

[14] R. F. Hyneman, "Closely-spaced transverse slots in rectangular waveguide," *IRE Trans. Antennas Propag.*, vol. 7, pp. 335–342, Oct. 1959.

[15] J. Liu, D. R. Jackson, and Y. Long, "Modal analysis of dielectric-filled rectangular waveguide with transverse slots," *IEEE Trans. Antennas Propag.*, vol. 59, no. 9, pp. 3194–3203, Sep. 2011.

[16] J. Liu and Y. Long, "Magnetic field integral equation for analyzing rectangular waveguide with periodic slots," *IEEE Trans. Antennas Propag.*, submitted for publication.

[17] C. J. Wang, C. F. Jou, and J. J. Wu, "A new two-terminal feeding active leaky-wave antenna," *IEEE Trans. Antennas Propag.*, vol. 46, no. 11, pp. 1749–1750, Nov. 1998.
[18] C. A. Balanis, *Advanced Engineering Electromagnetic*. New York: Wiley, 1989.
[19] A. A. Oliner and D. R. Jackson, "Leaky-wave antennas," in *Antenna Engineering Handbook*, J. L Volakis, Ed., 4th ed. New York: McGraw-Hill, 2007, ch. 11.

Analysis of a Conformal Archimedean Spiral Antenna Printed Within Layered Dielectric Cylindrical Media Using the Method of Moments

J. Wu, S. K. Khamas, and G. G. Cook

***Abstract*—A method of moments analysis of a conformal Archimedean spiral antenna is presented where the spiral is printed on a grounded cylindrical substrate with a superstrate. The layered cylindrical media are modelled using dyadic Green's functions in conjunction with novel asymptotic expressions to accelerate convergence. The results are validated against the limiting case of an equivalent planar structure as well as those obtained using commercial software.**

***Index Terms*—Conformal spiral antenna, cylindrical antennas, dyadic Green's function, method of moments (MoM), multilayered media.**

I. Introduction

Conformal antennas printed on a layered dielectric cylinder have been the subject of considerable research studies. For example, the radiation characteristics of cylindrical microstrip antennas [1]–[4] and a helical antenna printed on a dielectric coated perfectly conducting cylinder [5] have been investigated. Measurements and analysis of conformal patch arrays [6] and square spiral antennas above and in conformance with a perfectly conducting finite length cylinder have also been reported [7], [8], where the cylindrical ground plane has been modelled using a wire grid and the significance of the cylinder's length evaluated. In a subsequent paper, this analysis was used to design omni-directional circularly polarized arrays [9].

In the aforementioned studies, significant attention has been given to rigorous analysis using the method of moments (MoM), and to evaluation of the required dyadic Green's functions for cylindrical dielectric layers. Several articles have been published proposing procedures for the efficient calculation of these functions. For example, closed form Green's functions have been reported [10]–[12], where the discrete complex image theory (DCIM) and the generalized pencil of functions (GPOF) [13], [14] have been used. It was subsequently shown [15] that these Green's functions are slow to converge when both the source point (ρ', z', ϕ') and the field point (ρ, z, ϕ) are located on the same cylindrical radius $(\rho = \rho')$, and solutions to this problem have been proposed in several restudies [16]–[19].

In this article MoM analysis of a conformal Archimedean spiral antenna printed on a layered dielectric cylinder with a superstrate is presented, based on a previous study by the authors [19] in which the Green's functions have been calculated in closed form for increased computational efficiency. An investigation of this problem has not been reported earlier in the literature. Antenna properties such as input impedance, gain and axial ratio are calculated and validated against a CST Microwave Studio derived control [20]. In addition, the performance of the conformal spiral when printed on a large radius cylinder has been compared with that of an identical spiral printed on a planar substrate, and the effect of the PEC cylindrical core's radius on the axial ratio has been evaluated.

Manuscript received November 21, 2011; revised February 03, 2012; accepted April 02, 2012. Date of publication May 23, 2012; date of current version July 31, 2012.

The authors are with the Communications Research Group, Department of Electronic and Electrical Engineering, University of Sheffield, Sheffield S1 3JD, U.K. (e-mail: s.khamas@sheffield.ac.uk).

Color versions of one or more of the figures in this communication are available online at http://ieeexplore.ieee.org.
Digital Object Identifier 10.1109/TAP.2012.2201117

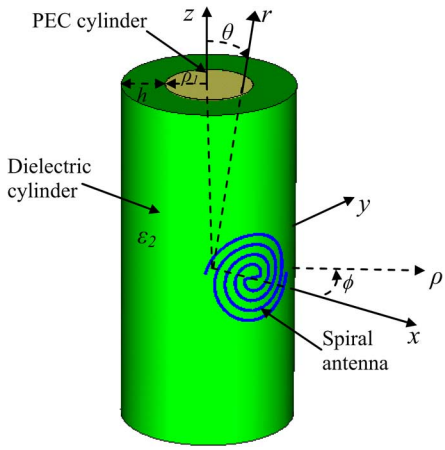

Fig. 1. Archimedean spiral printed on a layered cylinder.

II. Formulation

A. Spiral Conformal to a Cylinder

A printed cylindrical Archimedean spiral is shown in Fig. 1. There are three cylindrical layers in this structure; the innermost layer is a PEC cylindrical ground plane with a radius of ρ_1, the second layer is a substrate that has a dielectric constant of ε_2 and a thickness of h, and the third layer is free space. The overall radius of the layered cylinder is $\rho_s = \rho_1 + h$. We require an expression for the vector along the spiral arm $\underline{\ell}$ for integration of the method of moments basis and test functions in terms of the cylindrical geometry, where the corresponding unit vector $\hat{\ell}$ is defined as

$$\hat{\ell} = \hat{\ell}_z + \hat{\ell}_\phi. \tag{1}$$

The spiral function is given by

$$\Gamma = \Gamma_0 + a\psi \tag{2}$$

where a denotes the spiral constant and ψ the winding angle. For a planar spiral in the $y - z$ plane,

$$r_i = \Gamma_i \tag{3}$$

where r denotes a vector from the origin and i a Cartesian index. However, when the spiral is conformal to a cylinder as shown in Fig. 1,

$$r_x = \rho_s \cos\phi \tag{4a}$$
$$r_y = \rho_s \sin\phi \tag{4b}$$
$$r_z = \Gamma_z \tag{4c}$$

where

$$\phi = \frac{\Gamma}{\rho_s} \cos\psi. \tag{5}$$